# Solution of the many-electron many-photon problem for strong fields: Application to Li⁻ in one- and two-color laser fields

Theodoros Mercouris[1,*] and Cleanthes A. Nicolaides[1,2,†]

[1]*Theoretical and Physical Chemistry Institute, National Hellenic Research Foundation, 48 Vasileos Constantinou Avenue, Athens 11635, Greece*

[2]*Physics Department, National Technical University, Athens, Greece*

The solution of the many-electron many-photon (MEMP) problem for strong fields is facilitated if the corresponding theory entails a computational methodology that combines economy with accuracy and generality, as regards electronic structure and the incorporation of the continuous spectrum. By applying the nonperturbative MEMP theory (MEMPT) to the prototypical Li⁻ $^1S$ state, where both radial and angular correlations in the initial state and interchannel couplings in the final scattering states cannot be ignored, we computed frequency-dependent widths $\Gamma(\omega)$ of multiphoton detachment, as well as energy shifts $\Delta(\omega)$, for intensities $1 \times 10^9 - 1 \times 10^{11}$ W/cm², using one- as well as two-color fields. Even though the $1s^2 2p\ ^2P^o$ threshold is kept energetically closed, its coupling to the open channel $1s^2 2s\ ^2S$ cannot be ignored. For the two-color MEMP problem, the present application of the MEMPT provides results for a four-electron system, whereby the self-consistent field, electron correlation, and interchannel coupling are taken into account. The results for ($\omega$, $3\omega$) laser fields exhibit the recently predicted [Th. Mercouris and C.A. Nicolaides, Phys. Rev. A **63**, 013411 (2001)] linear dependence of the rate on cos $\varphi$, where $\varphi$ is the phase difference of the two weak fields. Based on this and on lowest-order perturbation theory (LOPT), we obtain a quantity characteristic of the system atom plus fields, which we name the "*interference generalized cross section.*" For the one-color system, comparison is made with our previous conclusions [C.A. Nicolaides and Th. Mercouris, Chem. Phys. Lett. **159**, 45 (1989); J. Opt. Soc. Am. B **7**, 494 (1990)] and with results from recent calculations of the two- and three-photon detachment rates by Glass *et al.* [J. Phys. B **31**, L667 (1998)], who implemented $R$-matrix Floquet theory, and by Telnov and Chu [Phys. Rev. A **66**, 043417 (2002)], who implemented time-dependent density-functional theory in the Floquet formulation via exterior complex scaling. Similarities as well as discrepancies are observed. Our results for $\Gamma(\omega)$ and $\Delta(\omega)$ involve a dense set of values as a function of $\omega$ and provide a clear picture of the physics below, at, and above the $3 \rightarrow 2$ photon threshold.

## I. INTRODUCTION

The interaction of a high intensity laser field with an atomic state leads to multiphoton ionization and shifts of the energy levels. From the theoretical point of view, one must expect that, just as in the case of one-photon absorption, the details of electronic structures and interchannel couplings in the initial and final states must leave their fingerprints on the observables, such as the rate of ionization or angular distributions of photoelectrons. Furthermore, real and virtual intermediate states play a role. And last but not the least, the physics must be described and computed by a practical theory that essentially accounts for the perturbation series of the total Hamiltonian to all orders. The totality of the above requirements defines a *many-electron many-photon* (MEMP) problem, a problem that appeared as soon as the possibility of measuring the effects of the interaction of atoms and molecules with strong laser fields emerged. Its solution necessitates the capacity of understanding and computing the significant features of the interelectronic correlations and of the atom-field interaction nonperturbatively. Furthermore, it is possible to expose the atom or the molecule to more than one

fields simultaneously. The ensuing complexity concerns both the type of necessary formalism and the method of computation.

Having the above in mind, in this paper we discuss the nonperturbative computation of the frequency-dependent rate of single electron multiphoton detachment of the Li⁻ $^1S$ state $\Gamma$ and the shift of its energy $\Delta$, when this state is exposed to a strong one-color field [$\Gamma(\omega)$, $\Delta(\omega)$] and to a weak two-color field with commensurate frequencies $\omega$ and $3\omega$, [$\Gamma(\omega,3\omega)$, $\Delta(\omega,3\omega)$], for three characteristic values of intensity: $1\times10^9$, $1\times10^{10}$, and $1\times10^{11}$ W/cm². We report the total electron detachment rates using frequencies in the range 0.011–0.021 a.u. For the two-color case we obtain numerically a quantity, characteristic of the system atom plus fields, which we name the "*interference generalized cross section.*"

The Li⁻ $^1S$ state represents a prototypical system where the multiconfigurational self-consistent field affects the zero-order orbitals and where radial as well as angular correlation cannot be ignored. Also, because of the low ionization limit, of the proximity of the $1s^2 2s\ ^2S$ and $1s^2 2p\ ^2P^o$ channels of the final neutral state and of the large dipole matrix element between them, it is possible on the one hand to have nonperturbative field-induced detachment at relatively low intensities, of the order of $10^{10}$ W/cm², and on the other to have significant influence from interchannel coupling. At the same

*Email address: thmerc@eie.gr

†Email address: can@eie.gr

time, because Li$^-$ has only four electrons, an *ab initio* treatment can be computationally economical, even if the corresponding solutions of the relevant equations have to be achieved with physically significant accuracy.

In the following section, we discuss briefly the published work on the MEMP problem for Li$^-$, which started with the first polyelectronic treatment of Refs. [1] and [2]. Earlier theoretical investigations from the polyelectronic point of view had involved only the relatively simple H$^-$ system or the use of model potentials for atomic negative ions (ANIs) in $^1S$ states. The substance of the results of that work on multiphoton detachment rates (MPDRs), and its comparison with results obtained from first principles, was discussed in Refs. [1–3]. More recently, the systematics and analysis of the effect of electron correlation on MPDRs via the changes of the ANI outer orbital in the asymptotic region, a region that is essentially adjusted semiempirically when accurate model potentials are used, was presented in Ref. [4].

In Sec. III we review the MEMP theory (MEMPT) of the linear and nonlinear response of an atomic state to one or more (commensurate) monochromatic fields [5]. In Sec. IV we present our results for one color and for two colors and their comparison with the published ones for the one-color case. In Sec. V we comment on the exterior complex scaling technique and its conceptual connection to the basis-dependent state-specific theory for the solution of field-free or field-dressed complex eigenvalue Schrödinger equations. Section VI provides the synopsis of the discussion of the present paper.

## II. PREVIOUS WORK ON THE THEORY AND COMPUTATION OF THE NONPERTURBATIVE RESPONSE OF THE Li$^-$ $^1S$ STATE TO ONE-COLOR STRONG ac FIELDS

Regarding the nonperturbative calculation of the nonlinear response to a linearly polarized strong laser field, the Li$^-$ $^1S$ state was first treated as a four-electron system in Refs. [1] and [2]. It is worth pointing out that the system was treated in the presence of a dc field as well. The MEMPT that was applied tackles the problem as one of searching for the state-specific complex eigenvalue of a field-induced complex resonance state, where, unlike the Floquet complex coordinate rotation method, which was first introduced by Chu and Reinhardt [6] with application to hydrogen, the coordinates of the atom-field Hamiltonian are real. In the MEMPT, the non-Hermitian origin of the complex eigenvalue problem is due to the complex scaling of the coordinate of certain orbitals, a procedure that is necessary for the regularization of the field-induced resonance wave function. Emphasis is on the appropriate choice and optimization of the function spaces representing the localized and the asymptotic parts of the resonance (field-dressed) state. The latter is expanded in terms of both real and complex basis sets in order to account for the electronic structure of the remaining bound state as well as for the outgoing flux of electrons. Because it is based on advanced polyelectronic methods for optimal calculation of wave functions of ground or excited state of $N$-electron systems, the MEMPT provides a practical framework for the systematic and economical incorporation of electronic struc-

ture and electron correlation features and for the understanding of their interplay with the transition process of interest.

A number of conclusions were reported in Refs. [1–3,4] concerning the one-, two-, and three-photon detachment rates of Li$^-$, and of ANIs in general. For example, it was recognized that, in Li$^-$, nonperturbative effects appear at intensities of the order of $10^{10}$ W/cm$^2$. The measured [7] and semiclassically explained [7] oscillatory structure of one-photon detachment rate in parallel ac and dc fields was confirmed for the first time quantum mechanically [1]. Also, it was pointed out that "near the two-photon threshold, the calculations show structure due to ac-field induced $^1S$-$^1D$ interchannel coupling and shape resonances" (Fig. 1 of Ref. [1]). The significance of this type of interchannel coupling was emphasized again in our work on the multiphoton detachment of H$^-$ [4,8]. It is natural that its effects will show up in other ANIs and for properties that are even more sensitive to the mixing coefficients, such as angular distributions of photoelectrons.

The structure of the MEMPT also allows the direct calculation of the linear and nonlinear frequency-dependent energy shifts of the specific level under investigation. As regards the Li$^-$ $^1S$ state, this was demonstrated in Ref. [2], where the dynamic polarizabilities and hyperpolarizabilities were computed. A more systematic analysis and other references are given in the recent application to He [9].

If the time dependence of the laser pulse is to be taken into account, the MEMP problem must be solved in terms of the time-dependent Schrödinger equation (TDSE). The Li$^-$ $^1S$ state has again been used as the exemplar in the first application of the state-specific expansion approach to the solution of the TDSE with a time-dependent laser-atom interaction Hamiltonian [10]. As was stated in the abstract of Ref. [10], "...the results on above threshold ionization (ATI) for photon energy$=1.36$ eV demonstrate the effects of initial-state electron correlation and of final-state field-induced coupling of open channels (the Li $1s^22s$ $^2S$ and $1s^22p$ $^2P^o$), as a function of field intensity."

In more recent years, the growing interest in the MEMP problem has led a few groups to the choice of the Li$^-$ $^1S$ state for further investigations of the one-photon induced electron detachment, by different methods [11–13].

Specifically, Glass *et al.* [11] applied the "$R$-matrix Floquet theory" to calculate one-, two-, and three-photon detachment rates at intensities of the order of $10^9$–$10^{10}$ W/cm$^2$. An interesting finding is that "even at a fairly modest intensity of $10^{10}$ W/cm$^2$ a four-photon process becomes important due to the three-photon excitation of $a$ $^1P^o$ resonance at the $3s$ threshold accompanied by single-photon emission" (p. L673 of Ref. [11]). In general, the results of Ref. [11] differ from the recent ones of Telnov and Chu [13], which also differed from the our earlier ones [1,2]. The existence of these discrepancies was one of our reasons for pursuing the present one-color investigation.

Kamta and Starace [12] adopted a two-active-electron approach and solved the TDSE for a linearly polarized pulse by a technique that is full dimensional and accounts for core polarization. Their method allowed the calculation of rates as well of angular distributions of double electron ejection. As

they stress in their abstract, "our results for angular distributions indicate that following multiphoton double ionization by an intense laser field, electrons are predominantly ejected along the laser polarization axis; however, a significant number are ejected perpendicularly to this axis." The quantities studied in Ref. [12] are outside the scope of the present work. However, it is perhaps of interest to bring to attention that the emission of electrons perpendicular to the laser field polarization axis has also been seen experimentally and obtained from the solution of the TDSE in the case of single electron ionization [14,15].

Finally, Telnov and Chu [13] applied the Floquet formulation of the time-dependent density-functional theory (TDDFT) by implementing the *exterior complex scaling* technique (see Sec. V and Ref. [16]). One- and two-photon detachment rates, angular distributions, and energy shifts were calculated, the emphasis being on the two-photon process, for which five values of the laser frequency were used that cannot excite the threshold of Li $1s^2 2p \ ^2P^o$. The computations were done for three values of intensity; $1 \times 10^9$, $1 \times 10^{10}$, and $1 \times 10^{11}$ W/cm$^2$. For the rates and the shifts, Telnov and Chu did not compare with the earlier results of Refs. [1,2,11]. This is done here. We note that the DFT uses semiempirical potentials and has limitations as regards general applicability to arbitrary electronic structures. In addition, it should be expected that its incorporation into a formalism for multiphoton absorption will carry the general advantages as well as the disadvantages of the DFT as regards accuracy. We point out that for the He $^1S$ state, whose electronic structure is simpler than that of the Li$^-$ $^1S$ state, comparison of the results of the Floquet TDDFT for two colors [17] with those of the MEMPT [18] reveals discrepancies.

## III. PRESENT APPROACH: BRIEF REVIEW OF THE MANY-ELECTRON MANY-PHOTON THEORY (MEMPT)

The key features and computational steps of the MEMPT are as follows.

(1) The framework is time independent and employs the "*atom plus field*" Hamiltonian, which, in the dipole approximation for linearly polarized polychromatic light along the $z$ axis is, in a.u.,

$$H_{ac} = H_{atom} + \sum_m^{ncol} \omega_m \alpha_{\omega_m}^{\dagger} \alpha_{\omega_m}$$

$$- \frac{1}{2} \sum_m^{ncol} F_m z (e^{i\varphi_m} \alpha_{\omega_m}^{\dagger} + e^{-i\varphi_m} \alpha_{\omega_m}). \quad (1)$$

It is assumed that the atom interacts with ncol number of fields with $\omega_m$ frequencies. $\alpha_{\omega_m}^{\dagger}$ ($\alpha_{\omega_m}$) are the photon creation (annihilation) operators and $F_m$ are the corresponding field strengths (1 a.u. = $5.14 \times 10^9$ V/cm). The use of Eq. (1) results in the determination of cycle-averaged laser-induced properties.

(2) The problem of computing the nonlinear response to all orders is formulated as follows. We first note that when the total Hamiltonian $H_{ac}$ is formally projected onto the full spectrum of the field-free atom, the discrete and scattering stationary states are mixed according to the symmetry of the atom-field interaction. The diagonalization of this matrix must create perturbed states with energies shifted from those of the field-free spectrum. At the same time, the presence of the continuous spectrum implies the possibility of outgoing flux of electrons, i.e., of field-induced (by one or more photons) ionization. Both the energy shift and the ionization rate are functions of the frequency and intensity of the field. Following the complex eigenvalue state-specific theory of field-free atomic and molecular resonance states [16,19–21], it becomes clear that, once the appropriate resonance outgoing wave boundary conditions are imposed on a bound-scattering state mixture, the relevant Schrödinger equation becomes a complex eigenvalue matrix equation, where the imaginary part represents the rate of decay into the continuous spectrum, i.e., the rate of ionization.

The fundamental proposal of the MEMPT is that the field-induced, resonance state many-electron problem must be solved in three basic steps. In the first one, we must choose appropriate $N$-electron $L^2$ function spaces consisting of real as well as of complex one-electron basis sets. The superposition of these wave functions, denoted by $\Psi(\mathbf{r}; \boldsymbol{\rho}^*)$, is connected directly to the unperturbed wave function of the state of interest $\Psi_0(\mathbf{r})$. $\mathbf{r}$ symbolizes the real coordinates of electrons in bound states. The complex coordinate $\boldsymbol{\rho}^* = \mathbf{r} e^{-i\theta}$ is the coordinate in the orbitals representing the outgoing electron. For example, the MEMPT wave function for single-electron ionization is

$$\Psi(\mathbf{r}; \boldsymbol{\rho}^*) = \sum_{i,n} \alpha_{i,n}(\theta) |\Psi_i(\mathbf{r}_N); n\rangle$$

$$+ \sum_{j,n} b_{j,n}(\theta) |X_j(\mathbf{r}_{N-1}, \boldsymbol{\rho}^*); n\rangle \quad (2a)$$

with

$$X_j(\mathbf{r}_{N-1}, \boldsymbol{\rho}^*) = \Psi_j(\mathbf{r}_{N-1}) \otimes \varepsilon \ell(\boldsymbol{\rho}^*). \quad (2b)$$

The optimization of the bound states $\Psi_i(\mathbf{r}_N)$ and $\Psi_j(\mathbf{r}_{N-1})$ (in which all the orbitals are real), is done according to the state-specific theory of electronic structure [21]. $X_j$ denotes unbound states in the continuous spectrum represented by complex $L^2$ wave functions. $|n\rangle$ denotes the photon states. Expansion (2a) is the same as the one used in the monochromatic case, since the frequencies of the polychromatic field are considered commensurable. In general, the contribution of each term of Eq. (2a) to the energy shift and width depends on the various $\omega_m$ and $F_m$.

In the second step, the field-dressed non-Hermitian Hamiltonian matrix is constructed using $H_{ac}$ of Eq. (1), according to the physics of the problem. The form of this matrix and the method of solution of the ensuing complex eigenvalue equation are discussed in Refs. [2,5,8,9,18]. The complex eigenvalue of the MEMPT matrix contains the field-induced energy shift $\Delta(\omega)$ and width $\Gamma(\omega)$ from the field-free real energy.

The third step involves the repeated diagonalization of the MEMPT matrix as a function of the rotation angle $\theta$ of the type of expansion of the complex basis set, and of the number of photon blocks, until stability in the complex eigenvalue is obtained. This complex eigenvalue is written as

$$z_0 = E_0 + \Delta - (i/2)\Gamma, \tag{3}$$

where $z_0 \equiv z_0(\omega_1,\ldots,\omega_{\text{ncol}};F_1,\ldots,F_{\text{ncol}})$, $\Delta \equiv \Delta(\omega_1,\ldots,\omega_{\text{ncol}};F_1,\ldots,F_{\text{ncol}})$, and $\Gamma \equiv \Gamma(\omega_1,\ldots,\omega_{\text{ncol}};F_1,\ldots,F_{\text{ncol}})$. $\Delta$ and $\Gamma$ are, in general, small compared to the unperturbed energy $E_0$, and $z_0$ is connected to $E_0$ smoothly as a function of $\omega_m$ and $F_m$.

The final solution contains the mixing coefficients $\alpha_{i,n}(\theta)$ and $b_{i,n}(\theta)$ of Eq. (2a). Projection onto scattering states provides additional information concerning the continuous spectrum, such as the understanding of ATI in the presence of a dc field [22], or of angular distributions.

## IV. RESULTS

According to the discussion above, the bound state wave functions that were used for this application are: The Li$^-$ $1s^2 2s^2$ $^1S$ (initial state), and the Li $1s^2 2s$ $^2S$ and $1s^2 2p$ $^2P^o$ (thresholds for the final state). The first one was correlated accurately in the $L$ shell [2]. The $K$ shell was left frozen, represented by the numerical Hartree-Fock (HF) orbitals of the multiconfiguration HF [23] calculation for the zero-order wave function containing the $2s^2 \leftrightarrow 2p^2$ angular correlation: $\Psi_0^{\text{MCHF}} = 0.9328 \, \psi(1s^2 2s^2) + 0.3605 \psi(1s^2 2p^2)$. The remaining $L$-shell correlation was obtained by minimizing the total energy via the variation of nonlinear parameters in the analytic virtual orbitals representing single and double electron excitations [21]. The final wave function consisted of 43 terms giving an energy $E_0 = -7.455\,364$ a.u., in very good agreement with the result of the pioneering configuration interaction calculations of Weiss [24], $E = -7.4553$ a.u.

The neutral core wave functions, Li $1s^2 2s$ $^2S$ and $1s^2 2p$ $^2P^o$, were computed at the HF level, with energies $E(^2S) = -7.432\,726$ a.u., and $E(^2P^o) = -7.365\,07$ a.u. As before [1,2], the inclusion of both states is necessary, even if reaching the Li $1s^2 2p$ $^2P^o$ state requires a number of photons larger than the one required for the Li $1s^2 2s$ $^2S$ threshold. This is because they are close to each other with a large oscillator strength, and, in addition, the magnitude of the dipole operator matrix elements between the Li$^-$ $(1s^2 2p\varepsilon s, \varepsilon d)$ $^1P^o$ scattering states and the correlated wave function of the Li$^-$ $^1S$ ground state is significant. (Obviously, there are many more types of coupling matrix elements in the full matrix.) Below, we will show (Fig. 7) the difference that exists in calculations of $\Gamma(\omega)$ with and without the presence of the Li $1s^2 2p$ $^2P^o$ channel.

The final state wave functions consisted of a relatively large number of angular momenta and configurations:

$$1s^2 2s\varepsilon\ell \; ^1L, \quad \ell = 0,1,\ldots,10,$$

$$\text{radial of } \varepsilon\ell = r^n \exp(-\alpha r e^{-i\theta}),$$



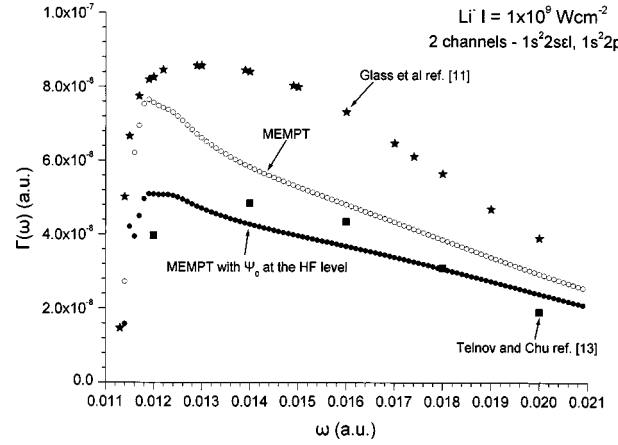FIG. 1. Theoretical results (in a.u.) for the rates of electron detachment from the Li$^-$ $1s^2 2s^2$ $^1S$ state by a linearly polarized laser field of intensity $I = 1 \times 10^9$ W/cm$^2$. For this intensity, the 3 $\rightarrow$ 2 photon threshold starts around $\omega = 0.0112$ a.u. Full stars: $R$-matrix Floquet theory, by Glass *et al.* [11]. Full squares: Floquet time-dependent density-functional theory via exterior complex scaling, by Telnov and Chu [13]. Open circles: Many-electron many-photon theory, this work. With electron correlation in the initial state and both the Li $1s^2 2s$ $^2S$ and $1s^2 2p$ $^2P^o$ Hartree-Fock wave functions for the description of the two cores of the continuum. Full circles: Many-electron many-photon theory, this work. Without electron correlation in the initial state (only the $1s^2 2s^2$ $^1S$ Hartree-Fock wave function is used).

$$1s^2 2p\varepsilon s \; ^1P^o, \quad 1s^2 2p\varepsilon p \; ^1S, \, ^1P, \, ^1D,$$

$$1s^2 2p\varepsilon d \; ^1P^o, \, ^1D^o, \, ^1F^o.$$

The parameters $\alpha$ and $\theta$ $(0 < \theta < \pi/2)$ are varied until stability in the result for the complex energy is observed.

### A. One color

Given the calculations of Refs. [1,10,11,13], we chose three values for the intensity: $1 \times 10^9$, $1 \times 10^{10}$, and $1 \times 10^{11}$ W/cm$^2$, and the range 0.011–0.021 a.u. for the frequency $\omega$. These sets of values cover the region of detachment by two and three photons without reaching the $1s^2 2p$ $^2P^o$ threshold. Of course, they include higher order multiphoton contributions. Since the one-photon detachment for low energy has been solved by a variety of methods, see Refs. [1,10,11,13] and references therein, we did not treat this case here.

The results are plotted in Figs. 1–7. In Figs. 1–6, we present the MEMPT results for the detachment rates and for the energy shifts that were obtained using only the HF wave function for the Li$^-$ $^1S$ state and the ones that were obtained by including electron correlation in this state. In Fig. 7 we show the MEMPT results without and with the presence of the Li $1s^2 2p$ $^2P^o$ channel.

As can be seen, the density of the calculated points in all figures is high, thereby allowing a clear definition of the curves. This is a result of the structure and methodology of the MEMPT, which allow economical computation without sacrificing accuracy.
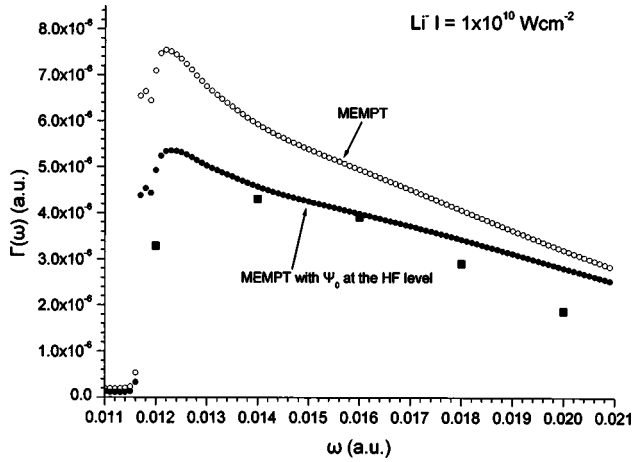
FIG. 2. For symbolism and comments, see caption of Fig. 1. Now, $I = 1 \times 10^{10}$ W/cm$^2$ and the $3 \rightarrow 2$ photon threshold starts around $\omega = 0.0115$ a.u.

Figures 1–3 show the widths (rates) in atomic units, as they were computed by Glass *et al.* [11], by Telnov and Chu [13], and by us. For $I = 10^9$ W/cm$^2$ (Fig. 1), the results of Ref. [11] for the two-photon rates are taken from their Fig. 3. It can be seen that just above the $3 \rightarrow 2$ photon threshold, the difference between the three computations is enhanced. The shape of the MEMPT curve indicates a faster reduction of the rate than either of the other two calculations. The results of the Floquet TDDFT treatment [13] are close to the MEMPT calculation when no initial state electron correlation is accounted for. We note that the MEMPT calculation at this level is rather simple. The most significant contribution of electron correlation is for frequencies close to the $3 \rightarrow 2$ photon threshold.

Figure 2 ($I = 1 \times 10^{10}$ W/cm$^2$) compares the MEMPT widths (without and with electron correlation in the $1s^2 2s^2$ $^1S$ state) with those of Telnov and Chu [13]. Note that now the $3 \rightarrow 2$ photon threshold is shifted slightly to higher frequencies. This shift becomes more pronounced at
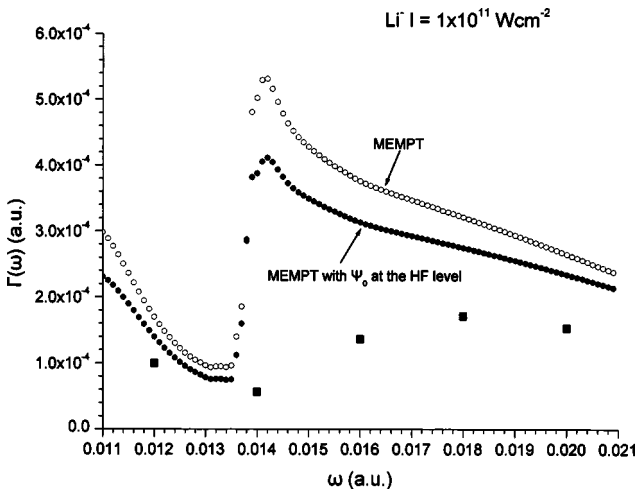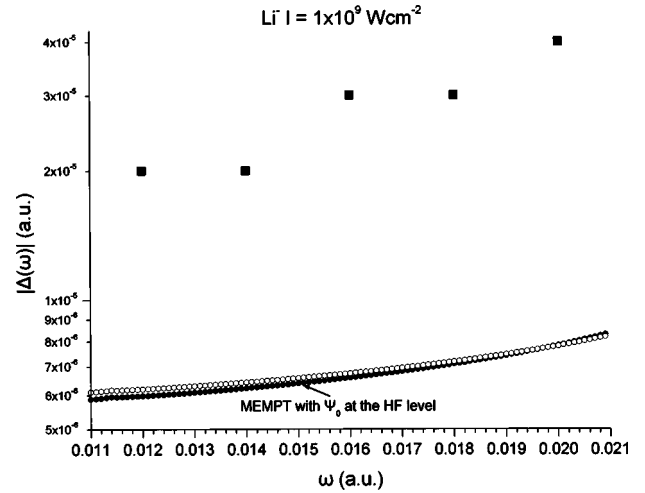


FIG. 4. Energy shifts for the Li$^-$ $1s^2 2s^2$ $^1S$ state, perturbed by a linearly polarized laser field of intensity $I = 1 \times 10^9$ W/cm$^2$. For symbolism and comments, see caption of Fig. 1.

$I = 1 \times 10^{11}$ W/cm$^2$ (Fig. 3). As before, the few Floquet TDDFT results are closer to the level of accuracy of the MEMPT without electron correlation.

Figure 3 ($I = 1 \times 10^{11}$ W/cm$^2$) shows not only a quantitative but also a qualitative difference between the MEMPT and the TDDFT results, the latter essentially missing the physics of the $3 \rightarrow 2$ photon threshold. Obviously, at this value of intensity, the demands on theory of the MEMP problem are such that a number of factors determining the physics have to be accounted for properly.

An equally dramatic difference, as the one of Fig. 3, between the MEMPT results and those of the Floquet TDDFT [13], is observed when comparison is made for the energy shifts $\Delta(\omega)$. These are shown in Figs. 4–6. The discrepancy is both qualitative and quantitative. It is worth pointing out that, as expected from first principles theory, the difference between the MEMPT correlated and uncorrelated results for the energy shifts is small for these intensities, and that both
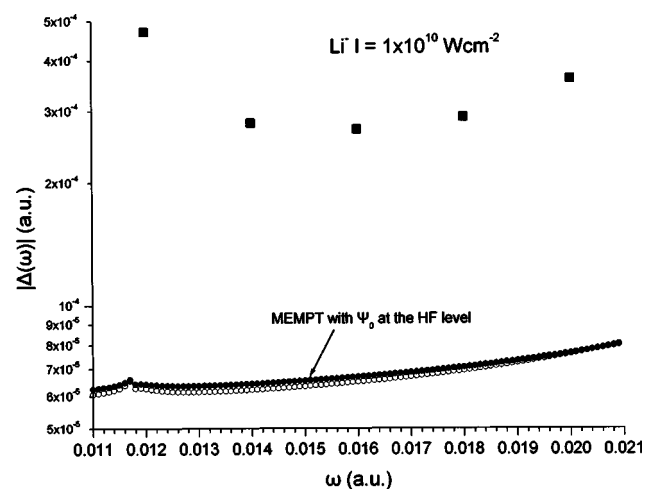


FIG. 3. For symbolism and comments, see caption of Fig. 1. Now, $I = 1 \times 10^{11}$ W/cm$^2$ and the $3 \rightarrow 2$ photon threshold starts around $\omega = 0.0135$ a.u.



FIG. 5. Energy shifts for the Li$^-$ $1s^2 2s^2$ $^1S$ state, perturbed by a linearly polarized laser field of intensity $I = 1 \times 10^{10}$ W/cm$^2$. For symbolism and comments, see caption of Fig. 1.
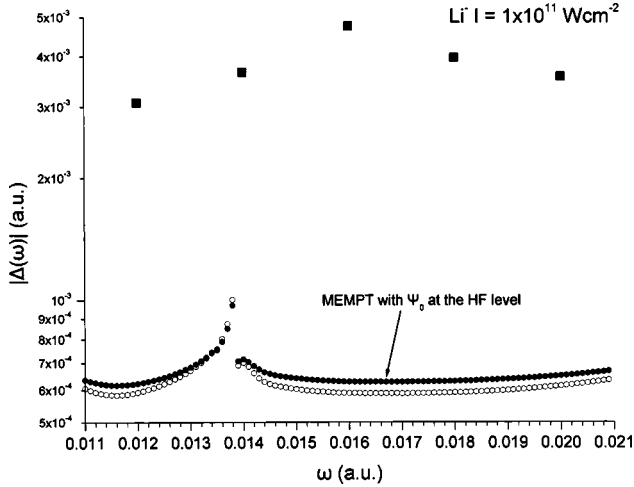
FIG. 6. Energy shifts for the Li$^-$ $1s^2 2s^2$ $^1S$ state, perturbed by a linearly polarized laser field of intensity $I = 1 \times 10^{11}$ W/cm$^2$. For symbolism and comments, see caption of Fig. 1.



FIG. 8. Two-color detachment rate for the Li$^-$ $1s^2 2s^2$ $^1S$ state as a function of cos $\varphi$, where $\varphi$ is the phase difference of the two fields. The linearity is discussed in the text [see Eq. (4)].

sets show the same smooth behavior and the same peak at threshold. The meaning of the few Floquet TDDFT values is unclear to us.

Figure 7 shows the MEMPT results for $I = 1 \times 10^{11}$ W/cm$^2$, without and with the presence of the $1s^2 2p$ $^2P^o$ channel. This figure demonstrates that, in cases of low-lying and field-coupled final core states, the inclusion of "closed" channels with specific characteristics is necessary if accurate results are to be obtained in a nonperturbative MEMP calculation. Such an inclusion characterizes the calculations of Refs. [1,2,10,11], but not of Ref. [13].

### B. Two colors, $\omega$ and $3\omega$: The interference generalized cross section

The structure of the MEMPT is such that it allows in a practical way the incorporation into the Hamiltonian of polychromatic fields with commensurate frequencies, see Eq. (1).
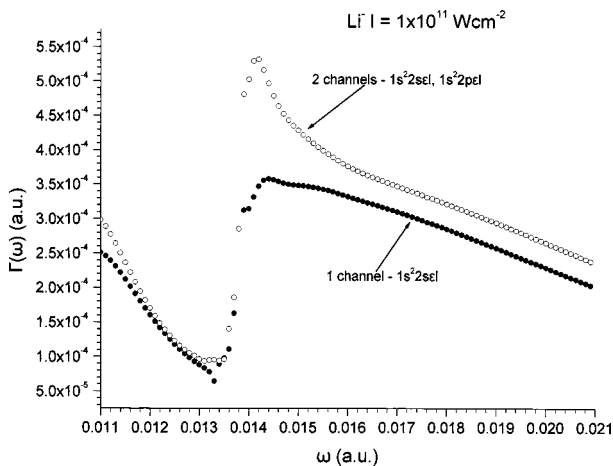


FIG. 7. The effect of the presence in the MEMPT calculation of the Li$^-$ $1s^2 2s^2$ $^1S \rightarrow$ Li $1s^2 2s$ $^2S$ two- and three-photon detachment rate, $\Gamma(\omega)$, in a.u., of the Li $1s^2 2p$ $^2P^o$ channel. The intensity of the linearly polarized laser field is $I = 1 \times 10^{11}$ W/cm$^2$.
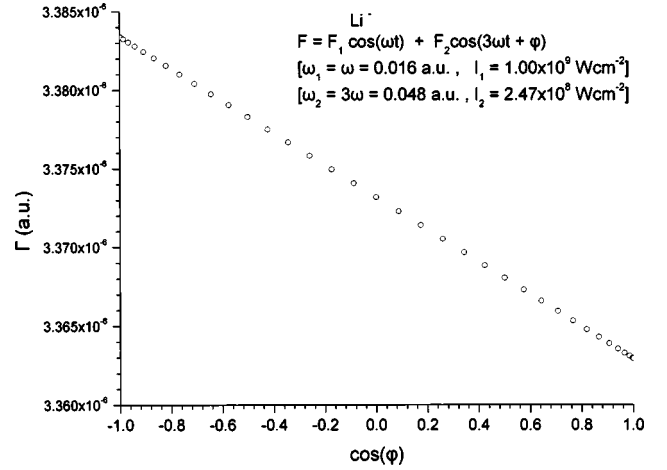
This has already been demonstrated in Refs. [5] and [18], with application to the He atom. The necessity of carrying out such computations reliably has to do not only with the production of new and experimentally verifiable results, but also with the problem of analyzing and controlling the ionization rate as a function of the variation of the phase difference $\varphi$ of the two fields. Through theoretical analysis, which focused on the interference of independent ionization paths to the continuous spectrum, we have already concluded that for weak fields, the rate $\Gamma(\omega, F_1; 3\omega, F_2, \varphi)$ must vary linearly with cos $\varphi$ [5]. This result, which may be taken as the equivalent of the results of lowest-order perturbation theory (LOPT) for one color, is verified again here from the application to the Li$^-$ state. Specifically, the results for $\omega = 0.016$ a.u., $I_1 = 1.00 \times 10^9$ W/cm$^2$, and $3\omega = 0.048$ a.u., $I_2 = 2.47 \times 10^8$ W/cm$^2$, are shown in Fig. 8. The dependence is linear, with a slope, $S(\omega, F_1; 3\omega, F_2)$, of $-1.023 \times 10^{-8}$. Given that the paths for one- and three-photon detachment for weak fields are independent and that the LOPT is valid, we calculate the quantity $I\sigma(\omega, 3\omega)$, which we name the "interference generalized cross section," as follows [valid for the particular choice of $(\omega, 3\omega)$ detachment],

$$I\sigma(\omega, 3\omega) = S(\omega, F_1; 3\omega, F_2)/F_1^3 \times F_2 \approx -2.5 \times 10^7 \text{ a.u.} \tag{4}$$

### V. COMPLEX SCALING IN THE MEMPT, AND EXTERIOR COMPLEX SCALING

The implementation of the TDDFT in the Floquet formulation was done by Telnov and Chu [13] by using a technique for regularizing matrix elements involving complex resonance eigenfunctions called "*exterior complex scaling*" (ECS). This technique was introduced into atomic physics in 1978 by Nicolaides and Beck [16a], and involves the procedure (Eq. 3 of Ref. [16a])

$$\int_{\text{all space}} \psi^2 dr = \int_0^R \psi^2 dr + \int_C \psi^2 ds, \qquad (5)$$

where $R$ is a point on the real axis at the edge of the inner region and $R < Res < \infty$. Equation (5) constitutes a practical regularization procedure for resonance wave functions that was written in response to criticism by Bransden [25] on the validity of a variational method for the complex energies of resonance states, proposed earlier by Nicolaides and Beck [26], and later applied to the computation of complex energies of dc-field-induced resonance states of the H atom [27]. Applications of Eq. (5), and of the notion implied by it, have been carried out by a number of researchers in atomic and molecular physics, the first one being the proposal by Simon [28] (who also provided the name *exterior complex scaling*) to treat molecular resonances in the Born-Oppenheimer approximation. A numerical determination using the ECS technique, of complex eigenvalues of resonances supported by a number of potentials, including the highly singular analytic Lennard-Jones potential and the numerically computed one for the $\text{He}_2^{2+} \, {}^1\Sigma_g^+$ state, was demonstrated in [16b].

Equation (2) of the MEMPT and Eq. (5) of the ECS method, have their origin in the idea that, regardless of whether the potential is of short or of long range, the crucial step in the understanding and calculation of the complex resonance eigenfunction is the $t=0$ localized wave packet $\Psi_0$ with a real energy $E_0$ (e.g., Refs. [20] and [29]). When the residual interaction dresses the state, the effect of the continuous spectrum is to turn $E_0$ into the complex eigenvalue of the resonance state satisfying the Schrödinger equation with the well-known complex outgoing wave boundary condition. To quote from Ref. [16b], "a significant part of the computation of a resonance of a given Hamiltonian can be done on the real axis with a suitable analytical or numerical method, and the regularizing complex scaling, yielding the decay information, can be done in the asymptotic region." When a basis set is used, as in the present application of the MEMPT, the continuation into the asymptotic region is done simply by the addition to the function space of real functions representing $\Psi_0$ (Hermitian system) of an optimized set of complex square-integrable functions. The system is thereby rendered non-Hermitian, expressing the physics of the outgoing electron flux as a function of frequency and intensity of the radiation.

## VI. SYNOPSIS

With the increasing capacity of carrying out quantitative measurements of observables resulting from the interaction of strong laser field with atoms and molecules, it is clear that the nonperturbative treatment of the MEMP problem is a basic requirement for theory. Although some useful information has been obtained from models or via semiempirical adjustments, it is preferable, just as in the case of the pure many-electron problem, to develop theory and computational understanding via methods that are based on first principles as regards electronic structure and the continuous spectrum.

The MEMP theory discussed and applied in this paper constitutes such an approach. It is nonperturbative and is applicable to situations with strong as well as weak, monochromatic or polychromatic, fields. It employs an accurate form of the atom plus field Hamiltonian in the dipole approximation [Eq. (1)], and it is an expansion-based approach [Eq. (2)], using as state-specific wave functions as possible [21]. The use of such an expansion makes it possible to monitor convergence and to understand quantitatively the interplay between the field-free spectrum, the electronic structure of the states involved, and the dynamics. Such wave functions can be obtained by the same methods for arbitrary electronic structures. It is worth noting that the extension to the relativistic domain is conceptually direct. The Hamiltonian of Eq. (1) can be modified accordingly while the calculation of state-specific wave functions (or variations thereof) can be achieved at the Breit-Pauli [21] or the Dirac-Coulomb [30] level.

The present application was concerned with the nonlinear response of the $\text{Li}^- \, {}^1S$ state to laser of one and of two commensurate colors. Our results are depicted in Figs. 1–8, where comparison with a few one-color results obtained by other methods [11,13] is also made.

The two-color MEMPT calculations are carried out for an $N$-electron ($N > 2$) system. The choice of a negative ion, where intermediate bound states are absent, allows for the possibility of computing efficaciously the effects of final state interference in a quantitative way. As in Refs. [5] and [18] for the multiphoton ionization rate of He, for weak fields there is a linear dependence on $\cos \varphi$ of the multiphoton detachment rate, where $\varphi$ is the phase difference between two fields with frequencies $[\omega,(2n+1)\omega]$.

---

[1] C. A. Nicolaides and Th. Mercouris, Chem. Phys. Lett. **159**, 45 (1989).

[2] C. A. Nicolaides, Th. Mercouris, and G. Aspromallis, J. Opt. Soc. Am. B **7**, 494 (1990).

[3] Th. Mercouris and C. A. Nicolaides, Phys. Rev. A **45**, 2116 (1992).

[4] C. A. Nicolaides, C. Haritos, and Th. Mercouris, J. Phys. B **33**, 2733 (2000).

[5] Th. Mercouris and C. A. Nicolaides, Phys. Rev. A **63**, 013411 (2001).

[6] S.-I. Chu and W. P. Reinhardt, Phys. Rev. Lett. **39**, 1195 (1977).

[7] H. C. Bryant, A. Mohagheghi, J. E. Stewart, J. B. Donahue, C. R. Quick, R. A. Reeder, V. Yuan, C. R. Humener, W. W. Smith, S. Cohen, W. P. Reinhardt, and L. Overman, Phys. Rev. Lett. **58**, 2412 (1987).

[8] C. Haritos, Th. Mercouris, and C. A. Nicolaides, Phys. Rev. A **63**, 013410 (2001).

[9] Th. Mercouris, S. I. Themelis, and C. A. Nicolaides, Phys. Rev. A **61**, 013407 (2000).

[10] Th. Mercouris, Y. Komninos, S. Dionissopoulou, and C. A. Nicolaides, Phys. Rev. A **50**, 4109 (1994).

[11] D. H. Glass, P. G. Burke, C. J. Noble, and G. B. Wöste, J. Phys. B **31**, L667 (1998).

[12] G. L. Kamta and A. F. Starace, Phys. Rev. A **65**, 053418 (2002).

[13] D. A. Telnov and S.-I. Chu, Phys. Rev. A **66**, 043417 (2002).

[14] C. Blondel, M. Crance, G. Delsart, and A. Girard, J. Phys. II **2**, 839 (1992).

[15] S. Dionissopoulou, Th. Mercouris, A. Lyras, and C. A. Nicolaides, Phys. Rev. A **55**, 4397 (1997).

[16] (a) C. A. Nicolaides and D. R. Beck, Phys. Lett. **65A**, 11 (1978); (b) C. A. Nicolaides, H. J. Gotsis, M. Chrysos, and Y. Komninos, Chem. Phys. Lett. **168**, 570 (1990).

[17] D. A. Telnov and S.-I. Chu, Int. J. Quantum Chem. **69**, 305 (1998).

[18] Th. Mercouris and C. A. Nicolaides, J. Phys. B **33**, 4673 (2000).

[19] C. A. Nicolaides, Y. Komninos, and Th. Mercouris, Int. J. Quantum Chem. **S15**, 355 (1981).

[20] I. D. Petsalakis, Th. Mercouris, G. Theodoracopoulos, and C. A. Nicolaides, Chem. Phys. Lett. **182**, 561 (1991).

[21] C. A. Nicolaides, Int. J. Quantum Chem. **60**, 119 (1996).

[22] Th. Mercouris and C. A. Nicolaides, J. Phys. B **24**, L57 (1991).

[23] C. Froese Fischer, Comput. Phys. Commun. **14**, 145 (1978).

[24] A. W. Weiss, Phys. Rev. **166**, 70 (1968).

[25] B. H. Bransden, Phys. Lett. **61A**, 145 (1977).

[26] C. A. Nicolaides and D. R. Beck, Phys. Lett. **60A**, 92 (1977).

[27] C. A. Nicolaides and H. J. Gotsis, J. Phys. B **25**, L171 (1992).

[28] B. Simon, Phys. Lett. **71A**, 211 (1979).

[29] C. A. Nicolaides, Phys. Rev. A **6**, 2078 (1972); C. A. Nicolaides and D. R. Beck, Int. J. Quantum Chem. **14**, 457 (1978).

[30] D. R. Beck, Phys. Rev. A **66**, 034502 (2002).